MICROSTRUCTURE AND TEXTURE EVOLUTION DURING HOT DEFORMATION OF AN AlMgSi-ALLOY

Tanja Pettersen and Erik Nes

Dept. of metallurgy, Norwegian University of Science and Technology,
N-7034 Trondheim, Norway.

ABSTRACT

An AA6060 alloy has been deformed in hot torsion at Zener-Hollomon parameters (Z) ranging from $Z=2\cdot10^{8}$/s to $Z=2\cdot10^{12}$/s and to various strains, ranging from $\varepsilon=1$ to $\varepsilon=25$, the resulting microstructures has been investigated by optical and electron microscopy and the texture evolution by X-rays. The stress-strain curves recorded during deformation showed an initial rapid rise to a peak flow stress, followed by a gradually softening to a final steady state plateau, this fall in flow stress has been discussed based on texturing effects and grain boundary sliding effects.

Keywords: *Large strain deformation, geometric dynamic recrystallisation, shear texture, torsion.*

1. INTRODUCTION

A large amount of work has been devoted to investigating the shape of the stress-strain curve during hot torsion deformation to high strains. The work has mostly been carried out on pure aluminium, from commercial grade to high purity aluminium. It has been found that the flow curve has a path not found in other deformation modes, increasing first to an initial, narrow steady state plateau, followed by a fall in flow stress to a final steady state. In the present investigation high strain deformation has been carried out on a 6060-alloy, special attention has been given to the development of the microstructure and in particular to the development of high angle boundaries. During deformation, the original grains changes their shape, and become elongated in the main deformation direction, and the surface area per unit volume of a grain increases with increasing strain. Grain boundaries often play an important role during nucleation of recrystallisation, and in the present work the shape change of the original grains has been studied.

2. EXPERIMENTAL

An AA6060-alloy (0.49wt% Mg, 0.42wt% Si, 0.20wt% Fe and balance Al) has been investigated in hot torsion, at temperatures and strain rates as listed in Table 1. Prior to testing the material was homogenised at 580°C for eight hours followed by water quenching. The initial grain size of the material was measured by optical microscopy to be ~100μm.

Table 1: A listing of the deformation conditions for the torsion tests carried out in the present investigation. In calculating Z an activation energy of 156kJ/mol has been used.

Z (1/s)	Temperature (°C)	Strain rate (1/s)	Strain
$2\cdot10^{8}$	528	0.01	1, 2, 4, 10
$2\cdot10^{10}$	520	1	1, 2, 3, 5
$7\cdot10^{11}$	480	10	1, 2, 3, 5, 25
$2\cdot10^{12}$	466	21	1, 2, 4, 10

Some of the samples were further investigated using optical microscopy, SEM, TEM, and X-rays. Because of the variation in strain throughout the specimen thickness, care must be taken when preparing the specimens for microstructural investigations. Specimens for optical microscopy and scanning electron microscopy (SEM) was ground and polished to a final thickness of 2.5-2.7mm, which ensures that the investigated area is at most 200μm below the surface. Samples for TEM

investigations were cut from the torsion specimens by spark machining to a maximum thickness of 600μm. These slices were then ground at both sides to a distance of 150-250μm from the surface, and finally electropolished. Samples for macrotexture analysis were prepared by removing the core of the torsion specimen, leaving a cylindrical wall of thickness 0.6mm to be ground and etched. ODF's were computed from four incomplete polefigures, which were measured by a Siemens D-5000 X-ray diffractometer.

3. RESULTS

Stress-strain curves from some of the experiments are displayed in Figure 1. At low strains there is a rapid rise in stress to an initial narrow plateau. This part of the stress-strain curve is consistent with similar experiments in other deformation modes. In torsion extra high strains are achievable compared to other deformation modes, and continuing straining the material reveals that this initial plateau only exists over a narrow region, followed by a gradually softening to a final steady state regime. The relative fall in flow stress for the different Zener-Hollomon parameters, $(\sigma_p-\sigma_\varepsilon)/\sigma_p$, was compared for the various Z-values. σ_p is the peak flow stress and σ_ε is the flow stress at strain ε. Some of the values found are displayed in Table 2.

Table 2: Decrease in flow stress at different strains for the investigated Z-values.

	Zener-Hollomon parameter (1/s)			
	$2\cdot10^{8}$	$2\cdot10^{10}$	$7\cdot10^{11}$	$2\cdot10^{12}$
$(\sigma_p-\sigma_{\varepsilon=5})/\sigma_p$	22%	20%	23%	23%
$(\sigma_p-\sigma_{\varepsilon=10})/\sigma_p$	34%	-	30%	33%

The table demonstrates that the relative fall in flow stress is independent of Zener-Hollomon parameter. In the specimen deformed to a strain of 25 the final steady state regime was reached at a strain of about 10, and after this strain only small changes in flow stress was observed.

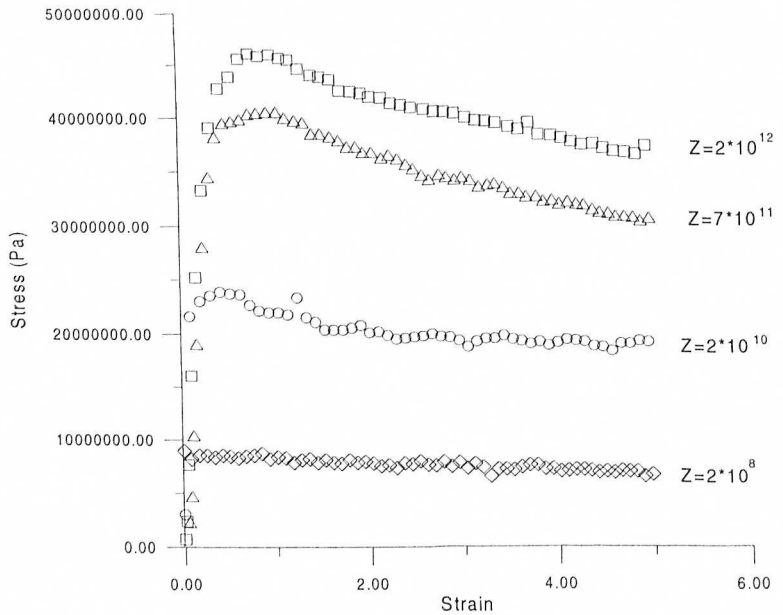

Figure 1: Representative stress-strain curves for AA6060 deformed at different temperatures and strain rates.

The textures obtained after deformation at $Z=7\cdot10^{11}$ to a strain of 3, 5 and 25 are shown in Figure 2. A typical shear texture, with a distinct ND-rotated cube is seen in Figure 2a) and b) (ND is the axis normal to the shear plane). These textures are representative for the textures measured at the lowest strains ($\varepsilon=1$ to $\varepsilon=5$) for both $Z=2\cdot10^{10}$ and $Z=2\cdot10^{11}$. The intensity of the textures, however, varies slightly and increases with increasing strain. To compare the textures obtained at different strains, the strength of the {001}<110>-component was measured for all strains. The usual convention is followed in the Miller index representation, that is, the {hkl} plane coincides with the shear plane and the <uvw> direction is aligned with the shear direction. The strongest texture was found at the highest Z-value, but the largest relative change in strength of the ND rotated cube at increasing strain was found at the lowest Z, with a strength of 4 times random at a strain of 1 increasing to a strength of 13 times random at a strain of 5. At $Z=7\cdot10^{11}$ the {001}<110>-component changed from a value of 8 times random at a strain of 1 to a value of 16 times random at a strain of 5. Changing the strain to 25 lead to a considerable change in texture, the intensity of the {001}<110>-component has decreased to a value of less than 2 times random. At the same time the fall in flow stress from the peak flow stress to a strain of 25 is about 30%, that is about 7% below the flow stress at a strain of 5.

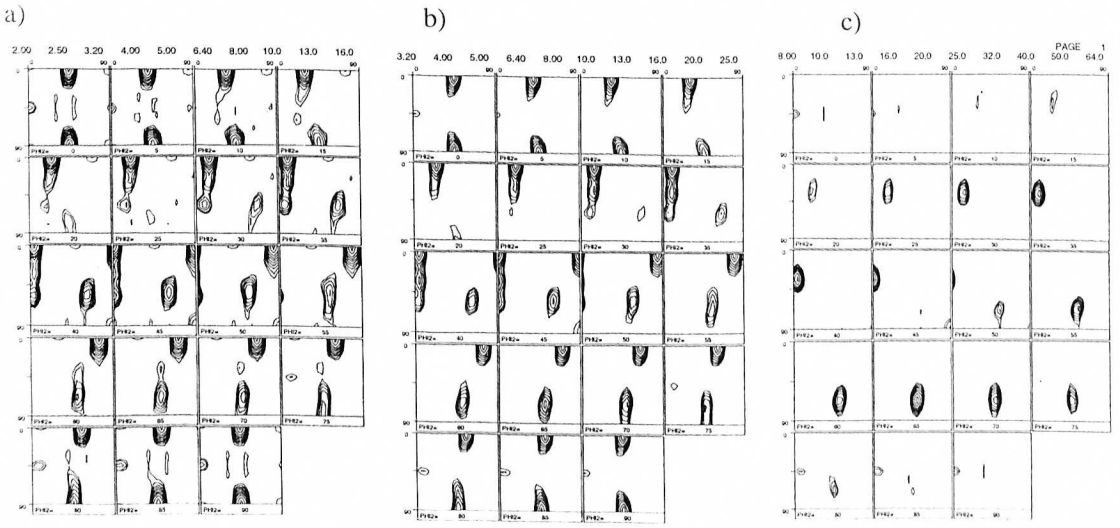

Figure 2: Texture (ODF) for material deformed in hot torsion at $Z=7\cdot10^{11}$, a) to a strain of 3, b) to a strain of 5, c) to a strain of 25.

Investigations using light optical microscopy showed that at low strains the original grains could be distinguished as separate entities, separated by the original grain boundaries, the grains were elongated in the shear direction, and the original boundaries were often found to have a serrated appearance. At increasing strain the grain structure is still elongated in the shear direction, but the original grains starts to break up, leading to a microstructure partly consisting of relatively small equiaxed grains surrounded by high angle boundaries. This type of structure is previously found in several investigations (e.g. McQueen et al. (1989)), an is often referred to as geometric dynamic recrystallisation (GDRX).

A more detailed investigation of the material has been carried out using SEM and TEM. Results from mapping experiments are shown in Figure 3, showing areas from specimens deformed to two different strains. At the lowest strain the original grains are clearly seen in the structure, and subboundaries are seen in the interior of the original grains (Figure 3a)). Higher strains results in a

structure where the original grains are not so distinct, and an increasing fraction of the subgrain boundaries are high angle boundaries (Figure 3b)).

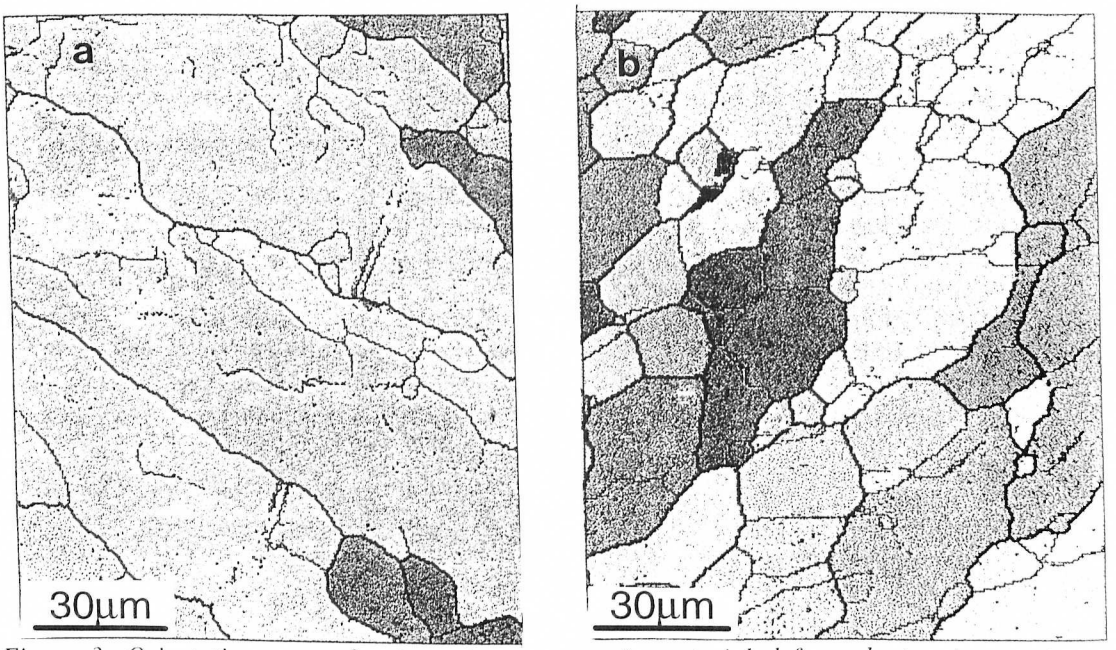

Figure 3: Orientation maps showing microstructure in material deformed at a temperature of 520 ℃ and a strain rate of 1/s, showing boundaries with a misorientation > 15 ° as heavy lines and misorientations > 1.5 ° as thin lines. a) Strain of 1, b) Strain of 3.

Measurements of subgrain sizes (δ) carried out in SEM and TEM are summarised in Table 3. The measurements at the lowest Z are carried out using SEM, and the measurements at the highest Z are carried out using TEM, which complicates comparison of the subgrainsizes, additional experiments using the material deformed at $Z=7\cdot10^{11}$ to a strain $\varepsilon=1$ was carried out using SEM, giving $\delta=4\mu m$.

Table 3: Mean intercept lengths (δ) measured in SEM and TEM.

	ε=1	ε=2	ε=3
$Z=2\cdot10^{10}$	5.5μm	5.6μm	5.4μm
$Z=7\cdot10^{11}$	3μm		3.4μm

4. DISCUSSION

At low strains (less than ~1) work hardening is dominating and leads to an increase in dislocation density and a rapid rise in stress. As the dislocation density increases the dynamic recovery reactions occurs at an increasing rate and the dislocations rearrange to form subgrain boundaries or annihilate. At a certain strain the work hardening and the dynamic softening reactions balance and an initial steady state flow stress is reached. Increasing the strain further leads to a drop in flow stress, not obtained in similar experiments performed in different deformation modes. The fall in the flow stress curve has by some authors (e.g. McQueen et al. (1985) and (1989)) been attributed to texturing which cause a change in the different texture components with increasing deformation. One of the components investigated by McQueen et al. (1989) was the {001}<110>-component, and for an initial grain size of 100μm (i.e. identical to the starting grain size in the present

investigation) it was found to change from a strong intensity at a strain of 3 to a very weak intensity at a strain of 20 which corresponded to the beginning of the final steady state part of the flow curve for the investigated material. Increasing the strain further (ε=60) was not reported to give a change in texture, that is, there was no change in the intensity of the {001}<110>-component along the final steady state regime. In the present investigation an increase in the intensity of the {001}<110> component was found with increasing strain in the decreasing-part of the flow curve (that is at strains ranging from ε=1 to ε=5). This is in accordance with the development predicted both by the full constraints Taylor model and the relaxed constraints Taylor model (Canova et al. (1984)). Increasing the strain to 25 gives a considerable change in texture, both as can be seen in Figure 2 and as indicated by a change in the intensity of the {001}<110>-component, which changes from a value of 15 times random at a strain of 5 to a value of less than two times random at a strain of 25.

The evolution of microstructure with strain was investigated by SEM and TEM and, rather surprisingly, no change in subgrain size was found with increasing strain from ε=1 to ε=3. In this interval the flow stress decreases with approximately 15%, which indicates an increasing subgrain size. The most prominent change in the microstructure with increasing strain was found to be that an increasing fraction of the boundaries turned into high angle boundaries. At small strain, when the material has reached the peak flow stress, the dislocations are arranged in a few high angle boundaries identical with the original high angle boundaries, in addition to being stored in a network of free dislocations, cell boundaries and subgrain boundaries of relatively low angle of misorientaion. Increasing the strain brings the free dislocations to collapse into boundaries with increasing misorientation, and the microstructure changes to a structure consisting of a large amount of high angle grain boundaries. This is illustrated in Figure 3b), showing an area from a specimen deformed to a strain of 3. These qualitative observations was further investigated by measuring the band width (the distance between high angle boundaries) at the different strains. The results are displayed in Figure 4. The line plotted in the figure shows the predicted distance between the original grain boundaries as a function of strain. This line is calculated using simple geometry and assuming constant volume of a grain during deformation:

$$D_a = \frac{D_0}{\sqrt{1+3\varepsilon^2}} \tag{3}$$

The distance between the original grain boundaries always has to be larger than or equal to the subgrain diameter, and above a certain critical strain ε_c, given by the following equation:

$$\varepsilon_c = \sqrt{\frac{(D_0/2\delta)^2 - 1}{3}} \tag{4}$$

the axial width of a grain changes from following Eq.3 to being a constant. (δ is the subgrain diameter, and pinch off is assumed to occur when the axial with reaches a value of 2δ). As can be seen from the figure, the measured values of the distance between the high angle boundaries are lower than that predicted from geometry, and in addition it is dependent on the Zener-Hollomon parameter. This indicates that high angle boundaries are created inside the original grains during deformation (grain break up). When the material reaches a strain of five, the measured distance between the high angle boundaries are close to the predicted value. Calculating the critical strain ε_c from Equation 4 using a subgrain size of 5.5μm (as measured by SEM for the material deformed at a Zener.Hollomon parameter of $2 \cdot 10^{10}$) we find a pinch off strain of ~5. At a strain of 5 the decrease in flow stress has reached 23%, and this part of the curve represent the steepest fall in flow stress.

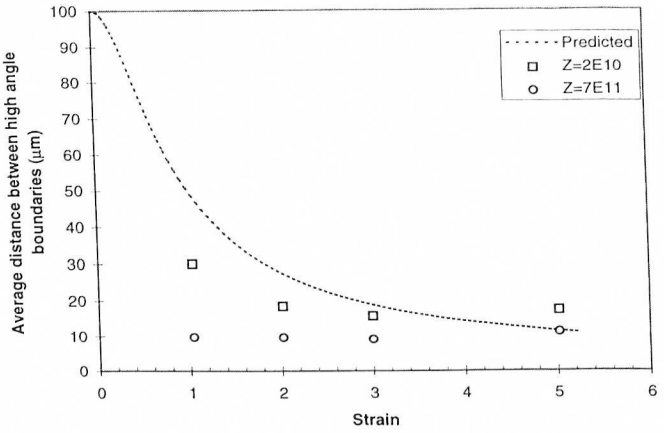

Figure 4: Axial band with as a function of strain. The squares and the circles show the values measured by EBSP, and the dashed line represents the geometrical predicted fall in axial with of a grain (for details, see text).

It has been suggested by some authors (e.g. Kassner et al. (1987)) that the decrease in flow stress is due to that a different deformation mechanism (grain boundary sliding) becomes operative. Grain boundary sliding is usually associated with high temperature deformation, i.e. during creep and especially superplastic flow it occurs by the motion of neighbouring grains along a common boundary. In the present investigation, as the strain increases the fraction of high angle boundaries become higher, and if grain boundary sliding occurs, the probability that it occurs increases with strain. An interesting possibility becomes that the fall in flow stress is caused by an increase in the amount of grain boundary sliding.

5. CONCLUDING REMARKS

It has been shown that the stress during torsion increases to a peak value followed by a decrease in flow stress to a final steady state value. The origin of this flow stress behaviour has been discussed taking into consideration texture effects and the effect of grain boundary sliding. In the present investigation the texture was not found to change in step with the changes in flow stress, in addition there was found no changes in subgrain size in the part of the flow curve with decreasing flow stress.

ACKNOWLEDGEMENTS

The authors wish to acknowledge Hydro Aluminium for financial support and for supplying the materials.

REFERENCES

[1] Canova G.R., Kocks U.F., Jonas J.J., Acta met., **32**, No.2, (1984), 211.

[2] Kassner M.E., McMahon M.E., Metal. Trans. A, **18**, (1987), 835.

[3] McQueen H.J., Knustad O., Ryum N., Solberg J.K., Scr. Metall., **19**, (1985), 73.

[4] McQueen H.J., Solberg J.K., Ryum N., Nes E., Phil. Mag. A, No. 60, **4**, (1989), 473.